Size and temperature dependence of the line shape of ESR spectra of the *XXZ* antiferromagnetic chain

Hiroki Ikeuchi,[1] Hans De Raedt,[2] Sylvain Bertaina,[3] and Seiji Miyashita[1,*]

[1]*Department of Physics, Graduate School of Science, The University of Tokyo, 7-3-1 Bunkyo-Ku, Tokyo 113-0033, Japan*
[2]*Zernike Institute for Advanced Materials, University of Groningen,*
Nijenborgh 4, NL-9747AG Groningen, The Netherlands
[3]*Aix Marseille Univ., CNRS, IM2NP UMR 7334, Marseille, France*

The electron spin resonance spectrum of the *XXZ* spin chain with finite length shows a double-peak structure at high temperatures around the electron paramagnetic resonance (EPR) frequency. This fact has been pointed out by direct numerical methods [S. El Shawish, O. Cépas, and S. Miyashita, Phys. Rev. B **81**, 224421 (2010); H. Ikeuchi, H. De Raedt, S. Bertaina, and S. Miyashita, *ibid.* **92**, 214431 (2015)]. The question of whether the double-peak structure survives in the thermodynamics is of particular interest. We study the size dependence of the line shape, including the even-odd effect. It is found that the peaks forming the double-peak structure are assigned to individual resonances, each of which is specified by the magnetizations of the resonating states $(M, M-1)$. To understand dependences, we decompose the spectrum into contributions from transitions specified by the magnetization, and we characterize the structure of the spectrum by individual contributions. We analyze the size dependence of each contribution individually by extending the moment method introduced by M. Brockman *et al.* to each component, and we find that the mean of each peak approaches the paramagnetic resonance point with $1/N$ (where N is the length of the chain), which indicates that the separation of the peaks of the double-peak structure also vanishes inversely with the system size. We also study the temperature dependence of the structure. At low temperatures, the spectrum has a single peak with a finite width at a position with a finite shift from the frequency of EPR, as pointed out by the analysis of field-theoretical works [M. Oshikawa and I. Affleck, Phys. Rev. Lett. **82**, 5136 (1999)]. The study of the temperature dependence of the spectrum shows how the high-temperature spectrum changes to the low-temperature one with a drastic broadening of the spectrum.

I. INTRODUCTION

Electron spin resonance (ESR) is one of the major tools used to obtain information about spin ordering. To understand the spectrum, the parameter dependence of a concrete ESR spectrum for a specified system has to be clarified, including the temperature dependence. To study these aspects theoretically, explicit forms of interactions of the magnetic structure of the system, such as the spatial configuration of magnetic ions in the lattice, must be taken into account. For example, modeling the ESR spectra of intrinsic defects in spin chains is an important problem for which data for finite but rather long chains are necessary [1]. Thus, it is necessary to develop a numerical method that can manage these long chains.

To study the temperature dependence, we may obtain the response $\chi''(\omega)$ by a direct numerical estimation of the Kubo fomula [2,3] for small systems for which we can obtain all the eigenvalues and eigenvectors of the system [4,5]. However, the method is inevitably limited to small systems. As a result, time-domain methods have been introduced in which the spectrum is obtained by Fourier transform of the autocorrelation function of magnetization (the AC method). It is known that the expectation value with the so-called random-weighted state or pure-quantum-thermal state $|\Phi\rangle$ yields an estimate of the trace of A, that is, $\langle\Phi|A|\Phi\rangle \simeq (\text{Tr}A)$, which becomes accurate for large-size Hilbert space D. Because

of this fact, there is no need to compute the average over the canonical distribution explicitly to obtain the thermal equilibrium average [6–11]. This approach has been used to study the temperature dependence of the total amplitude of the ESR spectrum for the single molecular magnet V_{15}, consisting of 15 $S = 1/2$ spins [8]. It is also known that finite observation time causes artificial modification of the spectrum (say, the Gibbs oscillation). In our previous study [12], we proposed a new method (the WK method) to make use of the Wiener-Khinchin relation with spectral density of magnetization fluctuation, in which the Gibbs oscillation is suppressed. However, at the same time, we found that that Gibbs oscillation is suppressed in a large system, and the AC method works efficiently. Thus, in the present work we obtained the spectrum using the AC method. With this method, we can study the double system size of the case of diagonalization theoretically. However, it is not the memory but the CPU time that prevents us from treating large systems. In the present paper, we calculated up to $N = 28$ in Sec. III. The methods are explained in detail in Ref. [12].

In addition to the direct numerical approach, for the resonance shift and the linewidth of the spectrum, which include basic information on the system, a lot of theoretical research has been conducted [13,14]. Oshikawa and Affleck developed an approach based on (1+1)-dimensional field theory, where they used the bosonization method and successfully derived the shift and the linewidth of the resonance peak at low temperatures in the thermodynamic limit [15]. This method has also been used successfully to investigate the effects of the edge state [16].

---

*Author to whom all correspondence should be addressed: miyashita@phys.s.u-tokyo.ac.jp

In the present paper, we study the one-dimensional $S = \frac{1}{2}$ *XXZ* model. It has been pointed out that the line shape of the *XXZ* spin chain with an even number of spins has a double-peak structure at high temperatures for lattices with finite length $N \leqslant 16$ [5], and we were interested in how the double-peak structure changes with the size of the system. The structure has been confirmed in systems with sizes up to $N = 26$ [12]. However, its detailed dependence on temperature and size is not yet known. Such information for finite sizes is important to study diluted systems that are an ensemble of short chains [1], where the temperature dependence of the spectrum is also important.

Thus, we study here the size dependence of the line shape not only for systems with even N where the double-peak structure appears, but also for systems with odd N where a single central peak with protuberances beside it appears.

To characterize the line shape, the so-called moment method has been introduced. In this method, we can obtain the strength, mean, and variance of the spectrum using the zeroth, first, and second moment of the spectrum. Maeda *et al.* derived the formula for the resonance shift defined by the first moment, which is exact up to first order in anisotropy, utilizing the integrability of the *XXZ* model [17]. By applying the Bethe ansatz technique, they obtained an analytic expression of the resonance shift over the entire temperature region. Brockmann *et al.* [18] also obtained consistent results, focusing on the moments of the spectral shape. In this way, a lot of information has been found with regard to the resonance shift and the linewidth. However, for the present problem of the explicit form of the shape of the spectrum, e.g., satellite peaks, long tails, etc., we need more detailed information.

In the present paper, we apply the moment method for each peak of the double peak or the protuberances. ESR takes place between the states that have magnetizations M and $M \pm 1$. It is found that groups of resonances forming the peaks are assigned to individual resonances, each of which is specified by the magnetizations of the resonating states $(M, M - 1)$. By making use of this fact, we decompose the spectrum into contributions from transitions specified by the magnetization, and we study the size dependence of each group by applying an extended moment method. With this analysis, we find that the deviation of the mean of the distribution for each group decreases as $1/N$. This observation strongly suggests that the structure would shrink to the center in the thermodynamic limit. Indeed, the numerical study up to $N = 28$ supports this dependence. On the other hand, we also find that its variance converges to a certain finite value even when N becomes large. Thus mathematically there is some possibility of a special shape of the spectrum in which the double peak may persist.

We also study the temperature dependence of the structure. As mentioned above, the high-temperature spectrum has a double-peak structure, the center of which is at the position of the electron paramagnetic resonance (EPR) frequency, i.e., $\hbar\omega_{\text{EPR}} = \gamma H$ (where γ is the gyromagnetic ratio). On the other hand, at low temperatures the spectrum has a single peak with a finite width at a position with a finite shift from the frequency of the EPR, as pointed out by the analysis of field-theoretical works [15]. The temperature dependence of the spectrum shows how the high-temperature spectrum changes to the low-temperature one with a drastic broadening of the spectrum.

The outline of this paper is as follows. In Sec. II, we introduce the model and method. In Sec. III, we study the size dependence of the structure of the spectra using numerical methods. In Sec. IV, we analyze the structure of the spectrum, decomposing it into contributions from transitions between specified sets of magnetizations. In particular, the estimation of the double peak's separation is an interesting problem, which is discussed in Sec. IV A. In Sec. V, the temperature dependence of the spectra is given. A summary and a discussion of related problems are presented in Sec. VI.

II. SYSTEM AND METHOD

We study a one-dimensional $S = \frac{1}{2}$ *XXZ* model in a static magnetic field H along the z axis,

$$\mathcal{H} = J \sum_{i=1}^{N-1} \boldsymbol{S}_i \cdot \boldsymbol{S}_{i+1} + \Delta \sum_{i=1}^{N-1} S_i^z S_{i+1}^z - g\mu_{\text{B}} H \sum_{i=1}^{N} S_i^z, \quad (1)$$

where Δ represents the strength of the anisotropy. Hereafter, we set $g\mu_{\text{B}} = 1$ for the sake of simplicity of notation. In this paper, we set $J = 1$ K, $\Delta = -0.08$ K (i.e., the *XY*-like anisotropy), and $H = 5$ K (i.e., a sufficiently strong field), and we impose the open-boundary conditions. We study the response, i.e., the complex susceptibility to an oscillating magnetic field parallel to the x axis: $\mathcal{H}_{\text{ext}} = \lambda_0 \cos\omega t \sum_{i=1}^{N} S_i^x$. In the present study, we do not include the dipole-dipole interaction, and thus the direction of the chain does not affect the results, although the dipole-dipole interaction could cause an interesting dependence of the spectrum on the angle between the lattice direction and the fields, such as the Nagata-Tazuke dependence [14].

Here let us recall important relations for the ESR spectrum. According to the Kubo formula [2,3], the ESR spectrum, i.e., the absorption rate $I^x(\omega)$ of the oscillating field, can be obtained with the dynamical susceptibility $\chi(\omega) = \chi'(\omega) + i\chi''(\omega)$ as follows:

$$I^x(\omega) = \frac{\omega\lambda_0^2}{2}\chi''(\omega), \quad (2)$$

$$\chi''(\omega) = \frac{1 - e^{-\beta\omega}}{2} \int_{-\infty}^{\infty} \langle M^x(0)M^x(t)\rangle_{\text{eq}} e^{-i\omega t}dt, \quad (3)$$

where $M^x(t) = e^{i\mathcal{H}t}M^x e^{-i\mathcal{H}t} = e^{i\mathcal{H}t}\sum_i S_i^x e^{-i\mathcal{H}t}$, and $\langle\cdots\rangle_{\text{eq}}$ denotes the thermal average with respect to $\mathcal{H}$ at a temperature β^{-1}. By using the set of eigenvalues and eigenvectors $\{E_n, |n\rangle\}_{n=1}^{D}$ of the Hamiltonian $\mathcal{H}$ (where D is the dimension of the Hilbert space of the Hamiltonian), $\chi''(\omega)$ is readily given by

$$\chi''(\omega) = \sum_{m,n} D_{m,n}\delta(\omega - \omega_{m,n}), \quad (4)$$

where

$$D_{m,n} \equiv \pi(e^{-\beta E_n} - e^{-\beta E_m})|\langle m|M^x|n\rangle|^2/Z,$$

$$\omega_{m,n} \equiv E_m - E_n, \quad Z = \sum_{n=1}^{D} e^{-\beta E_n}. \quad (5)$$
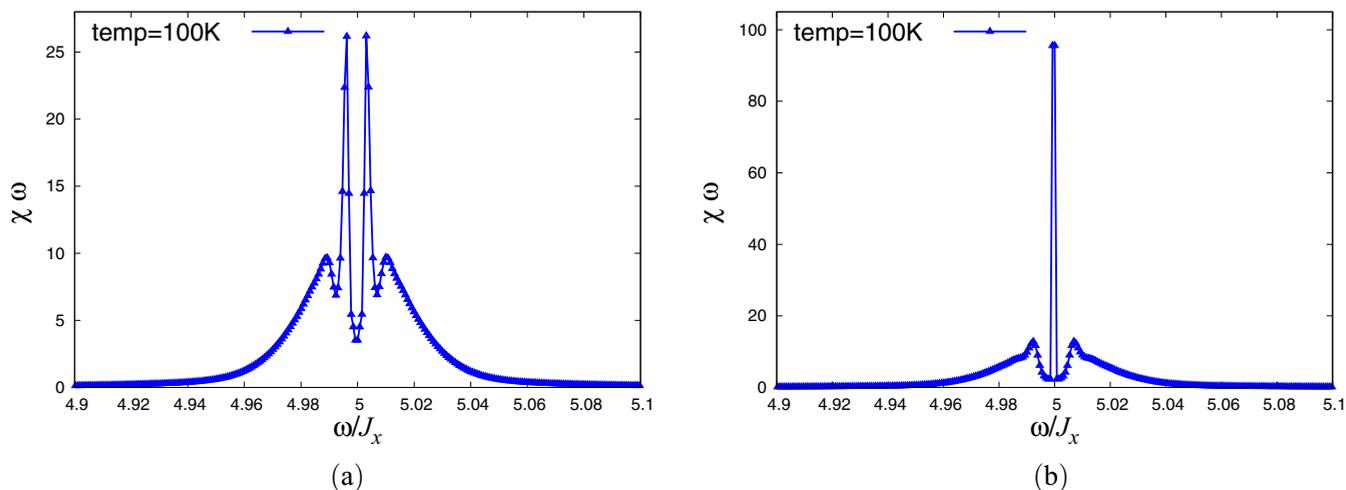
FIG. 1. The ESR spectra for (a) $N = 28$ and (b) $N = 27$ at $\beta^{-1} = 100$ K.

Hereafter, we use two types of numerical methods. For small systems, we obtain spectra using Eq. (5) by numerical diagonalization. For larger systems $N \geqslant 20$, we utilize the AC method [12], i.e., according to Eq. (3), we calculate the Fourier transform of the autocorrelation function in thermal typical states.

III. SIZE DEPENDENCE OF SPECTRAL SHAPES

As a typical example of the ESR spectra for odd- and even-number spins, we depict the spectra of $N = 28$ and 27 at a high temperature ($\beta^{-1} = 100$) in Figs. 1(a) and 1(b), respectively.

Now, we examine the size dependence of the characteristic shapes of the spectra, such as the double-peak structure. We depicted spectra of various sizes N in Figs. 2(a) and 2(b) for systems with even and odd numbers of spins, respectively. There we see a systematic size dependence. In the systems with even numbers of spins, the separation between double peaks $\Delta\omega$ decreases as the system size becomes large.

The nature of the shape in the thermodynamic limit is an interesting problem that has already been examined in Ref. [5].

The size dependence of the separation $\Delta\omega$ between the double peak is given in Fig. 3 (left). The error bars in the figure denote the mesh size of $\Delta\omega$ given by the observation time T as $2\pi/T$. We find that in even systems, the separation roughly decreases with the size as $1/N$. In Fig. 3 (center), we plot the size dependence of separations of two small protuberances of both the even and odd cases. This shows that the separation of protuberances decreases roughly proportionally to $1/N$. In Fig. 3 (right), we find that the heights of the peaks of protuberances increase with the system size.

We may anticipate that in the thermodynamic limit, the double peak may merge to become a single central peak. In addition, the separation between two small protuberances also seems to decrease with the increase of the system size, and it shrinks to the center in the thermodynamic limit. In fact, this problem has already been studied in Ref. [5] with inconclusive results. Below, we will study the size dependence by making use of the decomposition of the spectrum into components specified by the group of resonances with the magnetizations $(M, M - 1)$ between which the resonance takes place.
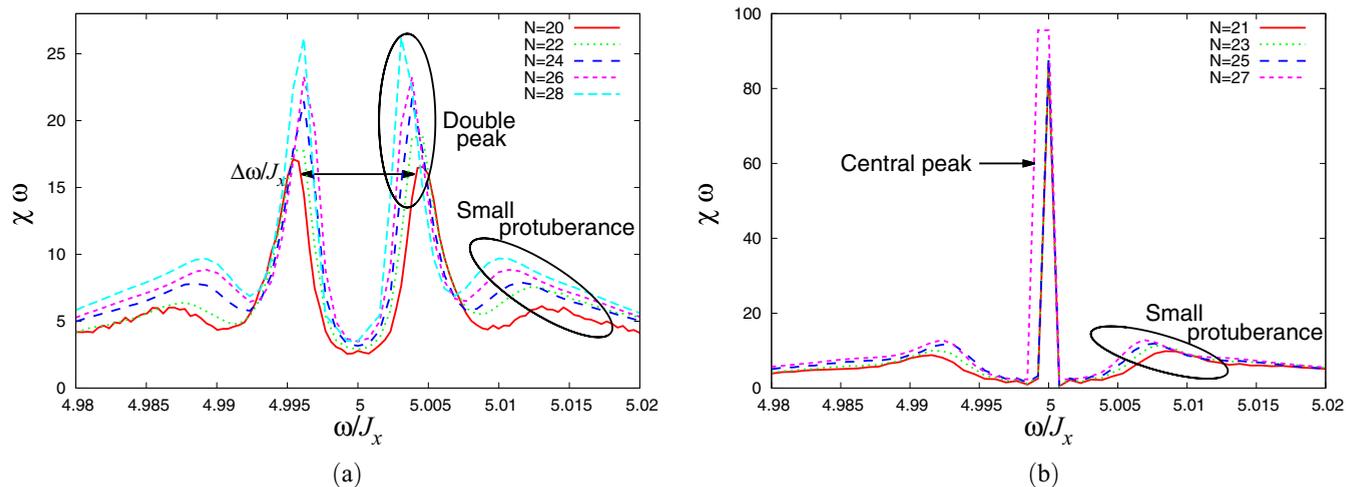
FIG. 2. (a) Spectra of systems with an even number of spins, $N = 20, 22, 24, 26$ and 28, depicted on the unified scale. (b) Spectra of systems with an odd number of spins, $N = 21, 23, 25$ and 27, depicted on the unified scale.
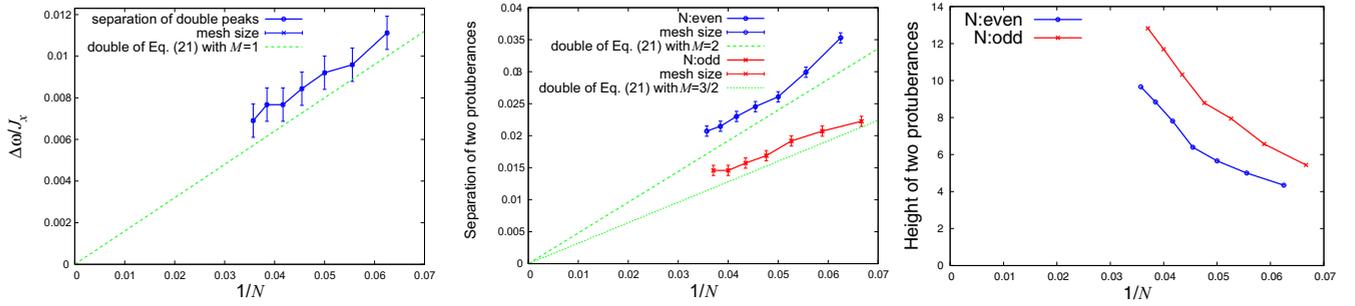
FIG. 3. (Left) Size dependence of the separation of the double peak in even systems. There seems to be a tendency for separation of the double peak to decrease as N becomes large. But it might be saturated at some point. The green line denotes theoretical values calculated by Eq. (21). (Center) Size dependences of the separation of two small protuberances. The red points denote odd-spin systems, and the blue points denote even-spin systems. We can find that the small protuberances come close to the center $\omega = H$ as the system size N increases. The error bars denote the mesh size of $\Delta\omega$ determined by the observation time T. The green lines denote theoretical values calculated by Eq. (21). (Right) Size dependences of the height of two small protuberances. The height is related to the the intensity of the absorption. The protuberances become larger with N increasing.

IV. DECOMPOSITION OF THE SPECTRUM INTO CONTRIBUTIONS FROM TRANSITIONS SPECIFIED BY MAGNETIZATION

In general, the resonance peaks in the ESR spectrum are given by the transition between states that have the magnetizations $\sum_{i=1}^{N} S_i^z = M$ and $M' = M \pm 1$ because $\langle M| \sum_{i=1}^{N} S_i^x |M \pm 1\rangle \neq 0$. Without the anisotropy ($\Delta = 1$), the system consists of an ensemble of multiplets of spin S each of which has the $(2S + 1)$ states with $M = -S, -S + 1, \ldots, S$. Although the system exhibits various interesting states, e.g., dimer, Haldane, and the spin-liquid state, etc., the spectrum has a single peak at the EPR position because the Zeeman effects of the external field H give simply the energy difference $\Delta E = g\mu_B H$ between the states of M and $M - 1$. Therefore, the structure of the high-temperature spectrum should be attributed to the energy structure lifted from the degeneracy by the anisotropy. The contributions from the transitions $(M \rightarrow M + 1)$ correspond to the emission, and they give the spectral weight at negative ω, which we do not consider here.

In what follows, we will scrutinize the mechanisms of the characteristic shapes observed in the previous section by focusing on the energy diagrams of the systems. The most dominant contribution comes from the transitions between levels within the same multiplet in the case of $\Delta = 0$. The breakdown of SU(2) symmetry due to Δ allows contributions from transitions between different multiplets, but the contributions from them are found to be very small. Thus, we will ignore those contributions in the interpretation of Fig. 5, even though these contributions are included in spectra obtained by the numerical method.

Since we are considering properties at high temperatures, instead of the susceptibility $\chi(\omega)$, which goes to zero as $\beta = 0$, we study

$$S_{xx}(\omega) = \int_{-\infty}^{\infty} \langle M^x M^x(t)\rangle_{eq} e^{-i\omega t} dt. \qquad (6)$$

Now we decompose the spectrum into contributions from transitions $(M \rightarrow M - 1)$ of various values of M. We denote

the group of resonances of $(M \rightarrow M - 1)$ by S_{xx}^M:

$$S_{xx}^M \equiv \int_{-\infty}^{\infty} \langle P_{(M^z=M)} M^x P_{(M^z=M-1)} M^x(t) P_{(M^z=M)}\rangle_{eq} e^{-i\omega t} dt, \qquad (7)$$

where $P_{(M^z=M)}$ is a projection operator that projects states onto the subspace where $M^z = M$.

For the systems with even N, the multiplets are with integer S. Each multiplet is separated into pairs of $\{M, -M\}$ and $M = 0$. Here we demonstrate the decomposition for a system with $N = 12$, because there are many states to form a continuous-like line shape, although we can still calculate the eigenstates by the exact diagonalization method.

In Fig. 4 (left), we show $S_{xx}^{M=1}$(solid line) [i.e., the contribution from the resonance of $(M = 1 \rightarrow M - 1 = 0)$] and $S_{xx}^{M=0}$ (dotted line) [i.e., that of $(M = 0 \rightarrow M - 1 = -1)$]. We find that $S_{xx}^{M=1}$ gives the right peak of the double peak, and $S_{xx}^{M=0}$ gives the left one. Here it should be noted that the contribution from each value of $S_{xx}^{M=0}$ gives a rather well-defined single peak.

We find that the double peak is given by the contribution of $S_{xx}^{M=1}$ and $S_{xx}^{M=0}$ [Fig. 4 (left)], the protuberances by $S_{xx}^{M=2}$ and $S_{xx}^{M=-1}$ [Fig. 4 (center)], and the others give the tail of the spectrum [Fig. 4 (right)]. The separation of the peaks according to M is attributed to the energy splitting due to the anisotropy Δ. To illustrate this, we draw the structure of the energy diagram as a function of static magnetic field. The number of states of a system with N spins is $D = 2^N$. For the large systems, D is too large to draw the diagram in a figure, and thus we draw the diagram for $N = 6$ in Fig. 5 (left) (green lines), which has $2^6 = 64$ lines. In the left panel, the detailed structure due to Δ is hardly seen, and hence the magnified structure is given in Fig. 5 (right). With the anisotropy $\Delta \neq 0$, the $(2S + 1)$ levels of a multiplet of spin S are split into a single state with $M = 0$ and S pairs of states that have opposite magnetization, i.e., $\{M, -M\} = \{1, -1\}, \{2, -2\}$, and $\{3, -3\}$ as shown by the red lines. The energy gap $\Delta E(M)$ between the doublets with $M = 1, -1$ and the single state with $M = 0$ at $H = 0$ is denoted by $\Delta E(1)$. $\Delta E(2)$ is the difference between the state $M = 2$ and 1 (or between the state $M = -2$ and -1)
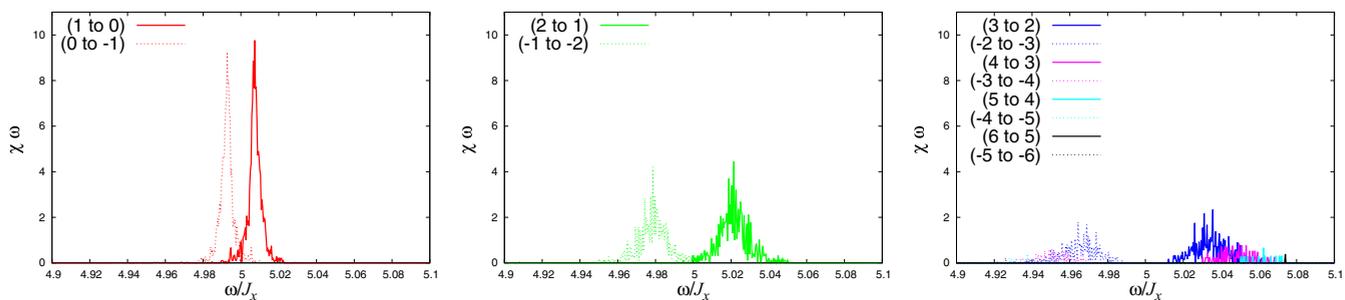
FIG. 4. Spectra for $N = 12$ S_{xx}^M classified by the magnetizations M of transitions at $\beta^{-1} = 100$ K. The left figure is for the spectrum by transitions $S_{xx}^{M=1}$(solid) and $S_{xx}^{M=0}$ (dotted). The center figure is for $S_{xx}^{M=2}$ and $S_{xx}^{M=-1}$. In the right figure, S_{xx}^M for larger M's are given: blue, $(3 \rightarrow 2)$, $(-2 \rightarrow -3)$; magenta, $(4 \rightarrow 3)$, $(-3 \rightarrow -4)$; cyan, $(5 \rightarrow 4)$, $(-4 \rightarrow -5)$; and black, $(6 \rightarrow 5)$, $(-5 \rightarrow -6)$.

and so on. Note that the amount of separation is given by $\Delta E(M)$.

We discussed earlier the multiplet with maximum spin $S = N/2 = 6$, but the pairs with $M = 1$ and 0 exist in all the multiplets of $S > 0$. Thus the number of transitions between $M = 0$ and ± 1 is maximum, and $S_{xx}^{M=1}$ and $S_{xx}^{M=0}$ have the largest contribution. At a finite temperature, the thermal population of the state of $M = 1$ is larger than that of $M = 0$ in the magnetic field, and thus $S_{xx}^{M=0}$ is larger than $S_{xx}^{M=-1}$. But at high temperatures, they are almost the same. The temperature dependence will be discussed later. The energy gaps $\Delta E(M)$ depend on the multiplet to which the states belong, and thus the resonance frequency is distributed as we see in Fig. 4 (left).

For an odd number of spins, the multiplets consist of half-odd spins S of $M = -S, -S + 1, \ldots, -1/2, +1/2, \ldots, S$. The transitions between $M = 1/2$ and $-1/2$ are the most populated, and the contribution of $S_{xx}^{M=1/2}$ gives the central peak. The contribution from others give protuberances and tails, just as for the case of even N.

A. Estimation of the size dependence of the spectrum for each M

Now, we examine the size dependence of the characteristic shapes of the spectra by making use of the moment method.

The method of moments originated in van Vleck's paper [19] and has been used as a basic tool to investigate the spectral shapes [2,20]. In a recent study [18], the moments of the whole spectrum for the XXZ chain in a wide temperature range were discussed in detail, the spectrum being regarded as a single peak and at a shifted position with a moderate width. The moment m_n of $S_{xx}(\omega)$ (6) is defined as [18]

$$m_n = \int_{-\infty}^{\infty} d\omega\, \omega^n \int_{-\infty}^{\infty} dt \langle M^x M^x(t) \rangle_{\mathrm{eq}} e^{-i\omega t} \qquad (8)$$

$$= 2\pi \langle M^x (\mathrm{ad}_{\mathscr{H}})^n M^x \rangle_{\mathrm{eq}}, \qquad (9)$$

where $\mathrm{ad}_{\mathscr{H}} \cdot \equiv [\mathscr{H}, \cdot]$. The intensity (i.e., the area of the spectrum), the mean position, and the linewidth are defined as

$$\text{intensity:} \quad m_0, \qquad (10)$$

$$\text{mean position:} \quad \frac{m_1}{m_0}, \qquad (11)$$

$$\text{linewidth:} \quad \sqrt{\frac{m_2}{m_0} - \left(\frac{m_1}{m_0}\right)^2}, \qquad (12)$$

respectively. Here we make some remarks about the definition of a linewidth given in (12). Indeed, (12) may not exist for the spectrum with an exact Lorentzian shape. But, as will be seen
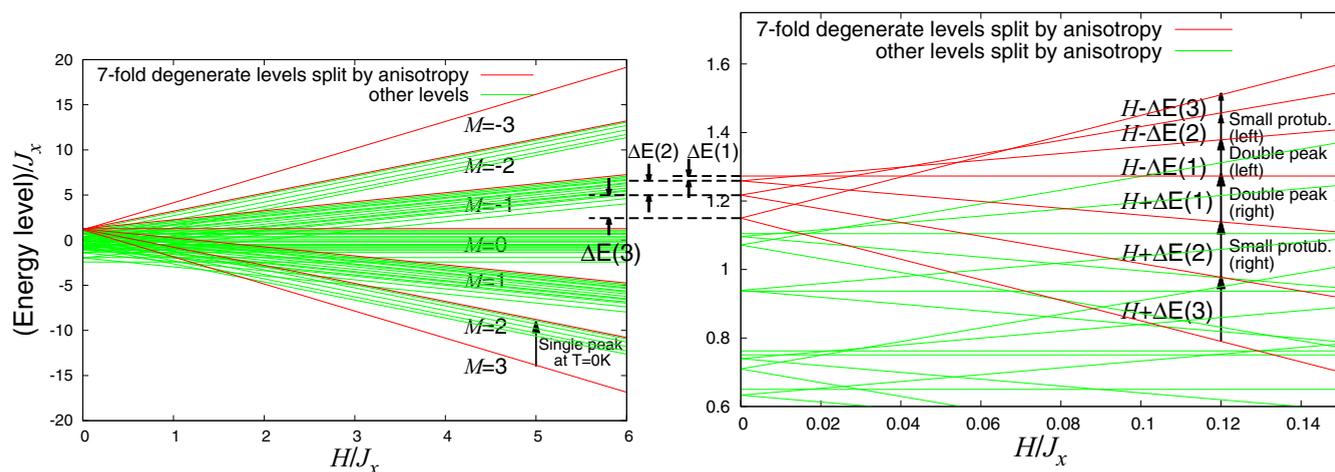
FIG. 5. (Left) 64 energy levels for a six-spin system. We accentuate the sevenfold degenerate levels by the red lines. (Right) An enlarged view of the left figure.

later, (12) always exists for the system we are considering, and it is known that (12) could be regarded as a good approximation to the width of the Lorentzian distribution in some situations [2,21]. In this sense, we adopt (12) as the definition of the linewidth, and other problems will be discussed in the last part of this section.

So far, the method has been used to study the whole shape of the spectrum. For our purposes, however, we need to improve this method because moments of the total spectrum are not very helpful in considering the detailed shape of the spectrum, such as the double peak. In other words, even if we know the moments with small values of n of the whole spectrum, we cannot derive the structure of the double-peak splitting.

1. Moment method for S_{xx}^M

Here, we make use of the property that we found in the previous section. The spectrum can be decomposed in contributions from transitions specified by the magnetization M (i.e., S_{xx}^M). Thus now we extend the method and investigate the properties of each S_{xx}^M to obtain information for the structure of the spectrum, e.g., the double peak. For example, if we know the mean positions of $S_{xx}^{M=1}$ and $S_{xx}^{M=0}$ given by the solid and dotted lines in Fig. 4 (left), respectively, we can estimated the separation of the double peak.

From now on, we set the external field $H = 0$, because the external field brings about just a shift of the mean position of the spectra, and it does not affect the shape (see Appendix).

The spectrum from the specified transition at $T = \infty$ is given by

$$S_{xx:T=\infty}^M$$
$$\equiv \int_{-\infty}^{\infty} \langle P_{(M^z=M)} M^x P_{(M^z=M-1)} M^x(t) P_{(M^z=M)} \rangle_\infty e^{-i\omega t} dt \tag{13}$$

$$= \frac{1}{2^N} \sum_{\substack{m \\ (M_m^z=M-1)}} \sum_{\substack{n \\ (M_n^z=M)}} |\langle m|M^x|n\rangle|^2 2\pi \delta(\omega - (E_m - E_n)). \tag{14}$$

Its nth-order moment is given by

$$m_n^M = \int_{-\infty}^{\infty} \omega^n S_{xx}^M(\omega) d\omega \tag{15}$$

$$= \frac{1}{2^N} \frac{\pi}{2} \sum_{\substack{\sigma \\ (M_\sigma^z=M)}} \langle \sigma|M^+ \mathrm{ad}_{\mathscr{H}}^n(M^-)|\sigma\rangle, \tag{16}$$

where $M^\pm \equiv M^x \pm iM^y$. As for the basis set $\{|\sigma\rangle\}$, we may use the up/down-spin representation, such as $|\uparrow\downarrow\downarrow \cdots \uparrow\downarrow\uparrow\rangle$.

In the infinite-temperature limit, the Boltzmann factor does not appear. Thus Eq. (16) can be calculated by counting the number of state (combinatorics). The zeroth-, first-, and second-order moments are written explicitly as

$$m_0^M = \frac{1}{2^N} \frac{\pi N}{2} \sum_{\substack{\sigma \\ (M_\sigma^z=M)}} \langle \sigma|S_1^+ S_1^-|\sigma\rangle, \tag{17}$$

$$m_1^M = -\frac{1}{2^N} \pi(N-1)\Delta \sum_{\substack{\sigma \\ (M_\sigma^z=M)}} \langle \sigma|S_1^+ S_1^- S_2^z|\sigma\rangle, \tag{18}$$

$$m_2^M = \frac{1}{2^N} \frac{\pi \Delta^2}{4} \left[(N-1) \sum_{\substack{\sigma \\ (M_\sigma^z=M)}} \langle \sigma|S_1^+ S_1^-|\sigma\rangle + 4(N-2) \sum_{\substack{\sigma \\ (M_\sigma^z=M)}} \langle \sigma|S_1^+ S_1^- S_2^z S_3^z|\sigma\rangle \right]. \tag{19}$$

From these quantities, we obtain the intensity (the area) of the spectrum, the mean position, and the linewidth of partial spectra from the transitions ($M \to M-1$) in the following:

$$m_0^M = \frac{1}{2^N} \frac{\pi N}{2} \binom{N-1}{\frac{N}{2}-M} \overset{|M| \ll N}{\sim} \sqrt{\frac{N}{2\pi}}, \tag{20}$$

$$\frac{m_1^M}{m_0^M} = (1-2M)\frac{\Delta}{N}, \tag{21}$$

$$\sqrt{\frac{m_2^M}{m_0^M} - \left(\frac{m_1^M}{m_0^M}\right)^2} = \frac{|\Delta|}{\sqrt{2}} \sqrt{\left(1-\frac{2}{N}\right)\left(1-\frac{(1-2M)^2}{N(N-1)}\right)}$$
$$\overset{|M| \ll N}{\sim} \frac{|\Delta|}{\sqrt{2}} + O\left(\frac{1}{N}\right). \tag{22}$$

Here we find the exact result that the center of the partial spectrum given by S_{xx}^M, which is located at a shifted position from the center at finite systems (i.e., to the right for $M \geqslant 1$ and to the left for $M \leqslant 0$), reduces to zero as $1/N$. This new exact property strongly suggests that the separation of the double peak reduces with N, although the separation is defined by the difference of the peak positions but not the difference of the mean. It should also be noted that these results are valid for any Δ and J.

2. Estimation of the separation of the double peak

Let us analyze the numerical results again from the viewpoint of Eqs. (20)–(22). The heights plotted in Fig. 3 (right) correspond to the intensity of the spectrum, and they relate to the quantity given by Eq. (20). Equation (20) indicates that the area of the partial spectrum increases with N, which supports the size dependence of the peak's height. Equation (21) is consistent with the observation of $1/N$ in the numerical results shown in Fig. 3 (left and center). We added the green lines represented as $2(1-2M)\Delta/N$ in Fig. 3. There are some differences between the numerical results and the green theoretical lines because Eq. (21) gives just the mean position, not the position of the maximum of the spectrum.
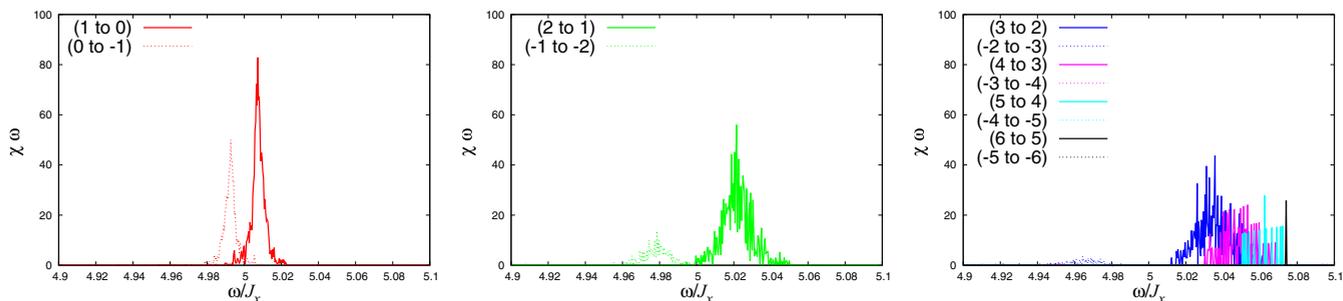
FIG. 6. Spectra for $N = 12$ classified by the magnetizations of transitions at $\beta^{-1} = 10$ K. The notation is the same as in Fig. 4. Here the asymmetry becomes significant because of the difference of the Boltzmann factors.

Nevertheless, the fact that the mean of the peak given by $S_{xx:T=\infty}^{M=0}$ goes to zero in proportion to $1/N$ strongly suggests that the peaks of the double peak shrink to the center together as $N \to \infty$. As for the central peak in odd-spin systems, its mean position turns out to always be zero by substituting $M = 1/2$ into Eq. (21).

V. TEMPERATURE DEPENDENCE
OF SPECTRAL SHAPES

As we explained above, the spectrum at high temperatures has a structure like the double peak around the EPR position. On the other hand, the field-theoretical study [15] gives a single peak at a shifted position from the EPR position with a width at low temperatures. Thus, it is interesting to study how the spectrum changes with the temperature. In this section, we investigate the temperature dependence of the ESR spectrum.

In the intermediate-temperature regime, the Boltzmann factors $\exp\left(-\beta E(H,m)\right)$ for $m = M$ and $-M + 1$ are gradually getting different. Consequently, $S_{xx}^{M>0}$ becomes larger than $S_{xx}^{-M+1\leqslant0}$, although the matrix elements are the same in both cases. Thus, the spectral shape is no longer symmetric around ω_{EPR}. We depict this change for partial spectra for specified values of $M = 1, 2, \ldots$ in Fig. 6 for $\beta^{-1} = 10$.

Now we study the temperature dependence of the whole spectrum. Let us first study the case in which the number of spins is even. The spectrum for $N = 20$ is depicted in Fig. 7.

In Fig. 7 (left), we find the spectrum at a high temperature ($\beta^{-1} = 100$ K), showing a double-peak structure and two small protuberances next to it, which were shown in the previous sections. The intensity is small because the prefactor of χ is proportional to β. As the temperature decreases, the intensity increases, and also the high-frequency side of the spectrum becomes dominant, as we explained above. Thus the spectrum shows a significant change with the temperature. At a low temperature ($\beta^{-1} = 1$ K), as shown in Fig. 7 (right), the spectrum has a single peak at a shifted frequency, which corresponds to the transition from the ground state with maximum magnetization, which is denoted by the arrow in Fig. 5 (left).

Next we study the case of an odd number of spins. In Fig. 8, the spectra for $N = 21$ are shown. The spectrum has a single sharp peak at the EPR position with protuberances beside it at the high temperature $\beta^{-1} = 100$ K. The central peak is a characteristic of the odd-number case. As the temperature is lowered, the spectrum changes to the high-frequency side. It should be noted that the intermediate temperature spectrum is very similar to the case of even spins ($N = 20$).

Here it should be noted that so far we have studied the case $H = 5J$, which is much bigger than other parameters, i.e., $H > \Delta, J$, because the spectrum shape does not depend on H but only shifts by H at high temperatures, and thus the choice of H is in a sense arbitrary and $H = 5J$ is convenient for the numerical calculation. In this field, the state with $M = S$ becomes the ground state, the excitation from which gives the
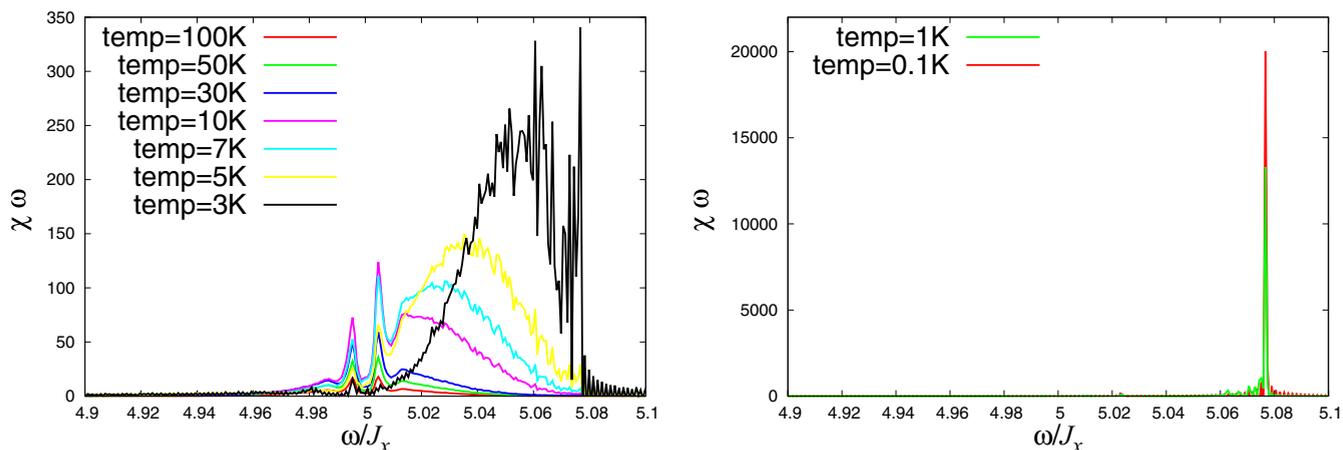
FIG. 7. The static magnetic field is set to $H = 5$ K. (Left) The spectra for $N = 20$ at $\beta^{-1} = 100, 50, 30, 10, 7, 5,$ and 3 K. (Right) The spectra for $N = 20$ at $\beta^{-1} = 1$ and 0.1 K.
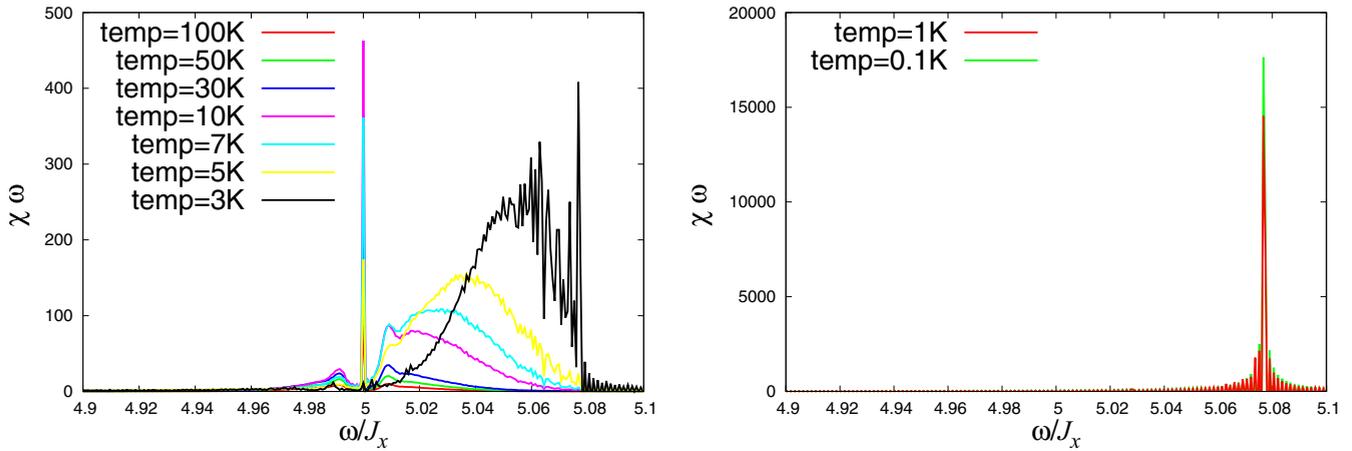
FIG. 8. The static magnetic field is set to $H = 5$ K. (Left) The spectra for $N = 21$ at $\beta^{-1} = 100, 50, 30, 10, 7, 5,$ and 3 K. (Right) The spectra for $N = 21$ at $\beta^{-1} = 1$ and 0.1 K.

dominant contribution at low temperatures. However, for the dependence of the spectrum on the temperature, the ratio of H and J also plays an important role.

Indeed, the interaction J is often bigger than the field H, and the situation that the field theory studied is the case $J > H > \Delta$. Also in this parameter regime, the field theory predicts a single peak at a shifted position at low temperatures [15]. But if $J > H$ is imposed, the magnetization is not fully polarized even at low temperatures, and therefore the single peak obtained above may not correspond to that obtained in the field theory.

Although the energy level distribution of our finite chain is not the same as that of an infinite chain, we may expect that to some extent it exhibits a qualitatively similar structure, because the present model contains properties up to the length $N = 20$. Thus, we study the temperature dependence for the case of a small value of H, say, $H = 0.5$ K, which is smaller than $J = 1$ K and still larger that $|\Delta| = 0.08$ K. The temperature dependence is depicted in Fig. 9. We find that qualitative features are similar to those of Fig. 7, i.e., the high-temperature structure moves to the high-frequency side similarly to that of Fig. 7, and at low temperature it tends to converge to a single

peak. However, the position of the peak is different from that of Fig. 7. We find that now the dominant peak is located at $\omega \simeq 0.511$ K. It is interesting that this value is consistent with the formula derived by field theory [15], i.e.,

$$\Delta\omega = -\frac{2}{\pi^2}\frac{\Delta}{J}\ln\left[\frac{J}{\max(T,H)}\right] \simeq 0.011 \text{ K.} \qquad (23)$$

From these observations, we would expect that the general tendency of the temperature dependence of the spectrum, i.e., the high-temperature spectrum changing to the single peak at a low temperature with a significant change at intermediate temperatures, would hold, and also that the chain of length of order $N \simeq 20$ may capture even quantitatively the general aspects of the temperature dependence.

VI. SUMMARY AND DISCUSSION

In the present paper, we studied the size and temperature dependence of the ESR spectrum for the *XXZ* chain. First, we investigated the size dependence of the separation of the double peak. The double-peak structure obtained by the AC method shows the tendency for the separation to shrink to zero
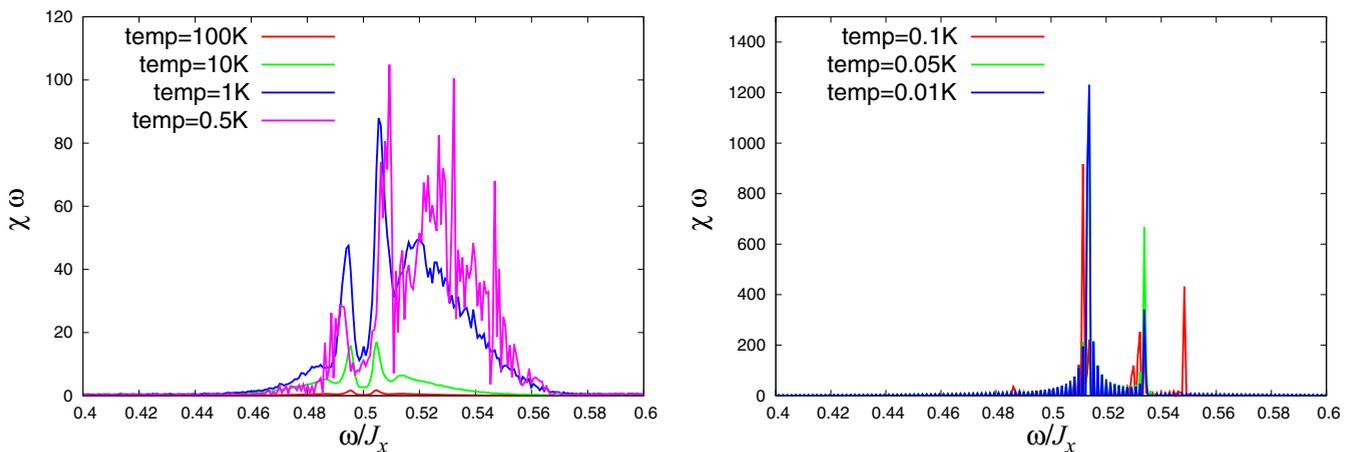
FIG. 9. The static magnetic field is set to $H = 0.5$ K. (Left) The spectra for $N = 20$ at $\beta^{-1} = 100, 10, 1,$ and 0.5 K. (Right) The spectra for $N = 20$ at $\beta^{-1} = 0.1, 0.05,$ and 0.01 K.
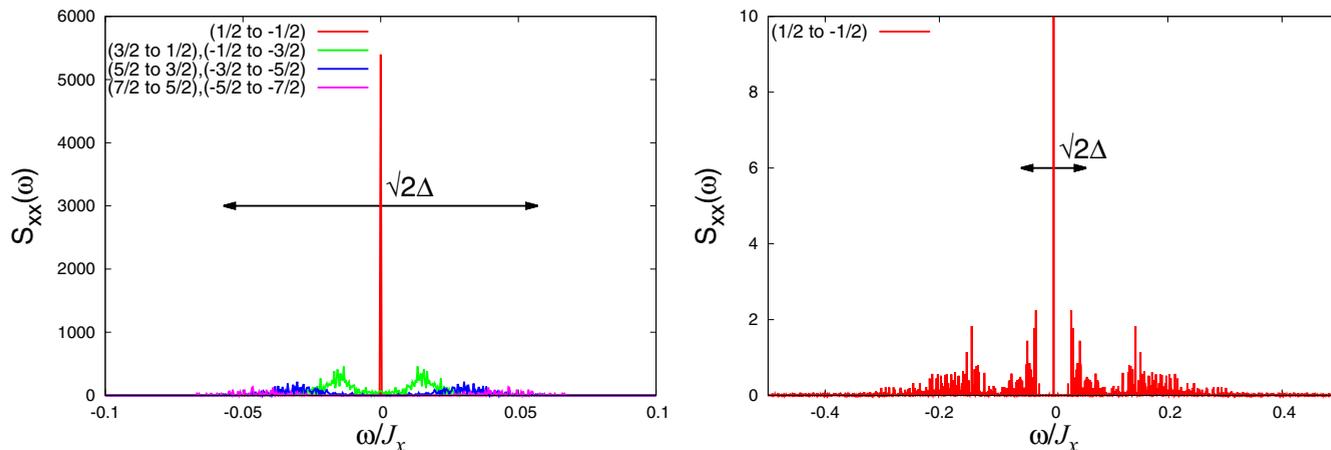
FIG. 10. (Left) and (Right) Spectrum for $N = 11$ and $\beta^{-1} = \infty$. Note that the scales are different between (Left) and (Right). According to Eq. (22), we consider $2 \times \Delta/\sqrt{2}$ as the linewidth, which is denoted by the black arrow.

as $N \to \infty$. The size dependence was analyzed by making use of an extended moment method. We found that the whole spectrum is decomposed into contributions of S_{xx}^M with various M and that each contribution of S_{xx}^M forms a single peak. By making use of these facts, we applied the moment method to each contribution of S_{xx}^M, and we found that the mean position of each spectrum exactly approaches the center as Δ/N, and becomes zero as $N \to \infty$. Thus, the separation of the double peak is expected to be estimated by the difference of means of corresponding peaks, i.e., S_{xx}^1 and S_{xx}^0, as shown in Fig. 2 (left). This fact strongly indicates that the separation of the double peak vanishes.

Now, we point out a delicate problem with the interpretation of Eq. (22), which stems from the fact that the variance of the distribution is of the order of Δ, which is finite. Indeed, the shape of the spectrum could be of any form within the range of Δ as long as the mean is zero. With this observation, small peaks away from the origin might give unexpected contributions, and we cannot exclude the possibility that in the thermodynamic limit, the double-peak structure remains present. To understand the role of the finite width, we study the single peak of $S_{xx}^{1/2}$ in odd-spin systems. In Fig. 10 (left), $S_{xx}(\omega)^{1/2}$ is shown for $N = 11$ together with other $S_{xx}(\omega)^M$. The width of the peak (red line) looks very small. The linewidth of the spectrum of $S_{xx}(\omega)^{1/2}$ calculated from Eq. (22) is shown by the arrow that is much larger, which seems contradictory to the data. To resolve this problem, we plot the spectrum on a different scale [Fig. 10 (right)]. We find small peaks far from the central peak, which cause the linewidth to be much broader than we expected. Therefore, in this sense, the linewidth calculated from Eq. (22) may not be appropriate to characterize the peak structure. For example, if we define the width by the width at half-maximum, the use of Eq. (22) is definitely an overestimation. Thus, when we consider that the structure consists of peaks of S_{xx}^M, the behavior of the mean would be more informative.

In the present paper, we strongly indicated the merging of the double peak in the thermodynamic limit. On the other hand, we would like to note that the double-peak structure is definitely present even for chains of considerable length ($N < 30$), and therefore the structure and its

temperature dependence may be accessible to experimental observation.

We also studied the temperature dependence of the spectrum. A drastic change from the high-temperature spectrum with a structure around the EPR position such as the double peak to the low-temperature spectrum with a single peak at a shifted position was observed. We found that the temperature dependence of the spectrum depends on the parameters, e.g., the field H and the anisotropy Δ. In the present paper we adopted $H = 5J$, which is much bigger than the anisotropy Δ and the interaction J, because the shape of the spectrum does not depend on H at high temperature, i.e., H simply shifts the center of the spectrum. However, the temperature dependence depends on H. In the situation that is treated in the field-theoretical approach, the condition $J \gg H > \Delta$ is imposed. To study the corresponding case, we studied the case $H = 0.5J$. We found that the general aspect of the temperature dependence is common, while the peak position at low temperature is different. We find that the numerical estimation of the shift of the system of $N = 20$ is rather close to that estimated by the field theory. This may indicate that $N = 20$ would already be a sufficient length to capture the general features of long chains. The temperature dependence of the line shape has not been studied in detail so far, and the drastic change with the temperature has not been thoroughly studied yet in experiment.

Finally, we add some comments regarding future works. In this paper, since we assumed the anisotropy to be small ($\Delta/J = -0.08$) and the transitions between different multiplets can be ignored, the decomposition of the spectrum into a contribution specified by magnetization is valid. However, the analytical results derived with the moment method in the preceding section are valid for any J and Δ, and in addition, according to our numerical simulation, the decomposition of the spectrum specified by magnetization somehow works well for the wide range of XY-like anisotropy ($0 < \Delta/J < 1$). On the other hand, for the Ising-like anisotropy ($\Delta/J > 1$), our method seems to be of limited use empirically.

The idea of the decomposition of the spectrum can also be used for other systems with magnetization conserved, e.g., systems with the Dzyaloshinskii-Moriya interaction whose

direction is parallel to the static field. These applications will be studied elsewhere.

APPENDIX: SPECTRAL SHIFT WITH AN EXTERNAL FIELD H

In Sec. IV A, we investigated the spectral shapes by calculating $S_{xx}(\omega)$ under no magnetic field, instead of the susceptibility $\chi''(\omega)$ under a finite static field H. This is valid for a sufficiently strong field $H \gg J(> 0)$ and a sufficiently high temperature $\beta \sim 0$. In this appendix, we illustrate this fact.

First, we consider the spectrum under a strong field H. Let the simultaneous eigenvectors of $\mathscr{H}_0 + \mathscr{H}'$ and $\mathscr{H}_z$ be $\{|E_n^0, M_n\rangle\}_{n=1}^D$,

$$(\mathscr{H}_0 + \mathscr{H}')\big|E_n^0, M_n\big\rangle = E_n^0\big|E_n^0, M_n\big\rangle,$$
$$\mathscr{H}_z\big|E_n^0, M_n\big\rangle = -HM_n\big|E_n^0, M_n\big\rangle, \qquad \text{(A1)}$$
$$n = 1, \ldots, D.$$

$S_{xx}(\omega)$ is given by

$$S_{xx}(\omega, H) = \frac{2\pi}{Z} \sum_{m,n} \big|\langle E_n^0, M_n|M^x|E_m^0, M_m\rangle\big|^2$$
$$\times \, \delta\{\omega - [(E_m - E_n) - H(M_m - M_n)]\}. \quad \text{(A2)}$$

Let us divide $S_{xx}(\omega, H)$ into two parts in the following:

$$S_{xx}(\omega, H) = S_{xx}^>(\omega, H) + S_{xx}^<(\omega, H), \qquad \text{(A3)}$$

where

$$S_{xx}^>(\omega, H) \equiv \frac{2\pi}{Z} \sum_{m,n} \frac{1}{4} \big|\langle E_n^0, M_n|M^+|E_m^0, M_m\rangle\big|^2$$
$$\times \delta\{\omega - [(E_m - E_n) - H(M_m - M_n)]\}, \quad \text{(A4)}$$

$$S_{xx}^<(\omega, H) \equiv \frac{2\pi}{Z} \sum_{m,n} \frac{1}{4} \big|\langle E_n^0, M_n|M^-|E_m^0, M_m\rangle\big|^2$$
$$\times \delta\{\omega - [(E_m - E_n) - H(M_m - M_n)]\}, \quad \text{(A5)}$$

and we find

$$S_{xx}^>(-\omega, H) = S_{xx}^<(\omega, H). \qquad \text{(A6)}$$

Noting that we are interested in the absorption, not the emission, we may focus on the region $\omega > 0$. The peaks in this region need to satisfy the relation $E_m - E_n > H(M_m - M_n)$. Then it follows that $M_m = M_n - 1$, because $H \gg J > 0$. Therefore, only $S_{xx}^>(\omega, H)$ contributes to the spectrum $S_{xx}(\omega, H)$ in the region $\omega > 0$:

$$S_{xx}(\omega, H) = S_{xx}^>(\omega, H), \quad \omega > 0, \qquad \text{(A7)}$$

$$S_{xx}(\omega, H) = S_{xx}^<(\omega, H), \quad \omega < 0. \qquad \text{(A8)}$$

According to Eqs. (A7) and (A4), we have $S_{xx}(\omega, H) = S_{xx}^>(\omega - H, 0)$. On the other hand, it is shown that

$$S_{xx}^>(\omega - H, 0) = S_{xx}^>(H - \omega, 0) = S_{xx}^<(\omega - H, 0), \quad \text{(A9)}$$

because of the symmetry of the shape of $S_{xx}^>$ as seen in Sec. IV, and Eq. (A6). Then, by using Eq. (A3), we have $S_{xx}^>(\omega - H, 0) = \frac{1}{2} S_{xx}(\omega - H, 0)$. Therefore, it follows that $S_{xx}(\omega, H) = \frac{1}{2} S_{xx}(\omega - H, 0)$, which is what we wanted to show.

The difference between $S_{xx}(\omega)$ and $\chi''(\omega)$ is just the presence of the factor $(1 - e^{-\beta\omega})/2 \sim \beta\omega/2$. $\chi''(\omega)$ vanishes at infinite temperature because of this factor, but we are interested in the spectral shape, not in the exact value of the peak. Therefore, we can ignore this factor and consider only $S_{xx}(\omega)$. Strictly speaking, the ω dependence of the factor $\beta\omega/2$ could deform the spectral shape, but this effect is also ignorable in the case in which H is very large.

[1] S. Bertaina, C.-E. Dutoit, J. Van Tol, M. Dressel, B. Barbara, and A. Stepanov, Phys. Rev. B **90**, 060404 (2014).

[2] R. Kubo and K. Tomita, J. Phys. Soc. Jpn. **9**, 888 (1954).

[3] R. Kubo, J. Phys. Soc. Jpn. **12**, 570 (1957).

[4] S. Miyashita, T. Yoshino, and A. Ogasahara, J. Phys. Soc. Jpn. **68**, 655 (1999).

[5] S. El Shawish, O. Cépas, and S. Miyashita, Phys. Rev. B **81**, 224421 (2010).

[6] P. de Vries and H. De Raedt, Phys. Rev. B **47**, 7929 (1993).

[7] T. Iitaka and T. Ebisuzaki, Phys. Rev. Lett. **90**, 047203 (2003).

[8] M. Machida, T. Iitaka, and S. Miyashita, J. Phys. Soc. **74**, 107 (2005); Phys. Rev. B **86**, 224412 (2012).

[9] A. Hams and H. De Raedt, Phys. Rev. E **62**, 4365 (2000).

[10] H. De Raedt, A. H. Hams, K. Michielsen, S. Miyashita, and K. Saito, Prog. Theor. Phys. **138**, 489 (2000).

[11] S. Sugiura and A. Shimizu, Phys. Rev. Lett. **108**, 240401 (2012); **111**, 010401 (2013).

[12] H. Ikeuchi, H. De Raedt, S. Bertaina, and S. Miyashita, Phys. Rev. B **92**, 214431 (2015).

[13] J. Kanamori and M. Tachiki, J. Phys. Soc. Jpn. **17**, 1384 (1962).

[14] K. Nagata and Y. Tazuke, J. Phys. Soc. Jpn. **32**, 337 (1972).

[15] M. Oshikawa and I. Affleck, Phys. Rev. Lett. **82**, 5136 (1999); Phys. Rev. B **65**, 134410 (2002).

[16] S. C. Furuya and M. Oshikawa, Phys. Rev. Lett. **109**, 247603 (2012).

[17] Y. Maeda, K. Sakai, and M. Oshikawa, Phys. Rev. Lett. **95**, 037602 (2005).

[18] M. Brockmann, F. Göhmann, M. Karbach, A. Klümper, and A. Weiße, Phys. Rev. B **85**, 134438 (2012).

[19] J. H. van Vleck, Phys. Rev. **74**, 1168 (1948).

[20] P. W. Anderson and P. R. Weiss, Rev. Mod. Phys. **25**, 269 (1953).

[21] J. Choukroun, J.-L. Richard, and A. Stepanov, Phys. Rev. Lett. **87**, 127207 (2001).